PRELIMINARY INVESTIGATIONS OF HIGH-FREQUENCY ATMOSPHERIC-PRESSURE PLASMA JET FOR ATOMIC EMISSION SPECTROMETRY

Martin ŠTĚPÁN[1], Martin SEMERÁD[2], Viktor KANICKÝ[3,*] and Vítězslav OTRUBA[4]

Laboratory of Plasma Sources for Chemical Analysis, Faculty of Science, Masaryk University Brno, Kotlářská 2, CZ-611 37 Brno, Czech Republic; e-mail: [1] woody@chemi.muni.cz, [2] semik@chemi.muni.cz, [3] viktork@chemi.muni.cz, [4] otruba@chemi.muni.cz

Received March 16, 2001
Accepted June 21, 2001

The 27.12- and 13.56-MHz plasma-jet discharges are generated in argon at atmospheric pressure. The plasma originates inside the nozzle of the bored metal power electrode and outflows against the counter-electrode. The discharge has a column shape with the diameter about 0.7–1.5 mm and the length 5–30 mm. The 27.12 MHz/100 W and 13.56 MHz/1 500 W generators are operated at a power of 100 and 200 W, respectively. Stable discharges are obtained within the range from 0.3 to 0.9 dm^3 min^{-1} Ar. The 27.12 MHz/100 W discharge is capable of accepting dry aerosol while the wet aerosol extinguishes this plasma. On the contrary, wet aerosol can be introduced into the 13.56 MHz/200 W plasma. The vibrational temperature of 3 000 K has been determined based on the intensity of the molecular band of the N_2 2nd positive system (365–383 nm) in the 27.12 MHz discharge. Intensity *vs* concentration dependences have been measured with Li 670.784, Na 588.995, Na 589.592, K 766.491 and Rb 780.023 nm lines. Limits of detection in the 27.12 MHz/100 W discharge coupled to an ultrasonic nebulizer with desolvation are 0.1 Li, 30 Na, 10 K and 3 ng cm^{-3} Rb. Limits of detection in the 13.56 MHz/200 W discharge connected to a pneumatic concentric Meinhard nebulizer is 8 ng cm^{-3} Li.

Keywords: Atomic emission spectrometry; AES; Plasma discharge; High-frequency plasma jet; Chemical analysis; Alkali metals.

Nowadays, the most frequently employed atmospheric plasma discharge for atomic emission spectrometry (AES) is the inductively coupled plasma[1] (ICP), which has been applied to inorganic elemental analysis for nearly four decades[2,3]. Besides the high temperature of the ICP discharge, it is its unique geometry, which is responsible for the most of its favourable analytical characteristics. The annular channel of the ICP allows efficient vaporization of a sample and subsequent atomization, ionization and excitation. Other flame-similar electrical discharges, such as direct-current plasma or microwave-induced plasma do not exhibit this central channel, which re-

doi:10.1135/cccc20011348

sults in limited sample-plasma interaction and less advantageous analytical properties. Although the exceptional properties of the ICP prefer this discharge to other atmospheric-pressure plasmas, the analyst should not forget potentials of other plasma sources, which are exhibiting further development[4]. Among others, a microwave-induced plasma based on microstrip technology has been recently developed and used for atomic emission spectrometry determination of mercury[5,6] and some non-metals[7].

A high-frequency (radio-frequency) plasma-jet discharge (RPJ) operated in argon under atmospheric pressure has been designed originally for physical studies[8]. One of the properties of this discharge is the ability to be operated in liquid environment, which is appreciated yet in non-analytical applications[9–11]. So far this discharge has been used for treatment of archaeological artifacts in solutions. The system appears to be promising for industrial applications, such as cleaning of surfaces or thin film depositions at atmospheric pressure[11].

This work describes construction of laboratory-made plasma-jet system capable of stable long-term operation. A special effort is aimed at reaching the configuration and operating conditions of the plasma jet at which the discharge tolerates an introduction of analytical sample. Measurements concerning the influence of the geometric configuration and operating conditions on the shape, temperature and long-term stability of the discharge are presented. A considerably important step consists in searching a suitable nebulizing system and testing the robustness of the discharge by the aerosol introduction. The significance of this potential source for AES stands out particularly from the viewpoint of reduction of working gas consumption and power input. Moreover, miniaturization of the whole device should not be omitted. The discharge is optimized for the determination of alkali metals.

EXPERIMENTAL

Generators

Two high-frequency (*hf*) generators have been employed in this work. The 27.12-MHz generator has been originally assembled during the experiments described in refs[8–10]. This generator can stand a long-term operation at maximum 100 W. In this work we term this generator the *low-power* device. For our purposes, we have provided this generator additionally with a tuning unit Versa Tuner MFJ-969 (MFJ Enterprises, Inc.), which allows the impedance matching with the plasma discharge. By means of this tuner, the ratio of forwarded and reflected power is kept as high as possible[12].

The 13.56-MHz generator PM 101 is a commercial device (International Plasma Corporation, U.S.A.). This generator is routinely used in our laboratory as a power supply for the

commercial low-pressure oxygen-plasma ashing device, which is employed for decomposition of samples with organic matrices. This generator, denoted in our work as the *high-power* device, can be operated at most at 1 500 W. As a matching unit, the digital antenna tuner HFT 1500 (VCI Vectronics™, Valor Enterprises, Inc.) has been employed. Schematic drawing of the experimental arrangement is given in Fig. 1. Operating conditions of both generators are presented in Table I.

TABLE I
Operating conditions of plasma discharges

Generator type	Low-power	High-power
Working frequency, MHz	27.12	13.56
Maximum generator power, W	100	1 500
Maximum load of tuning cell, W	300	3 000
Forwarded power, W	100	200
Reflected power, W	2–5	10–30
Argon flow, $dm^3\ min^{-1}$	0.3–1.2	
Nitrogen flow, $dm^3\ min^{-1}$	0.0–0.8	
Time constant of measurement, s	0.1–1.0	

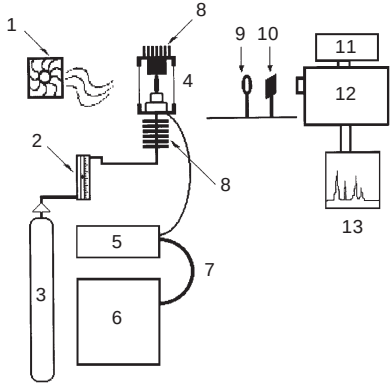

FIG. 1
Schematic drawing of the experimental setup: 1 air fan, 2 flowmeter, 3 working gas-pressure cylinder, 4 chamber with jet, 5 antenna tuner, 6 RF power supply, 7 coaxial cable, 8 ribbed cooler, 9 lens, 10 filter, 11 amplifier, 12 monochromator, 13 strip-chart recorder

Discharge Chamber and Sample Introduction Systems

In spite of the surface treatment utilization[8–11], the analytical application of the plasma-jet requires stable cofiguration with a counterelectrode. For this purpose, a discharge chamber has been constructed which also allows to maintain a steady and controllable ambient atmosphere[12]. A schematic drawing of the discharge chamber is given in Fig. 2. The power electrode consists of a bored brass rod provided with an interchangeable conical tip (15 × 6 mm) with central capillary nozzle 0.5–1.5 mm in diameter. Brass, copper and graphite were studied as materials for this tip. The power electrode is connected through the matching unit to the *hf* generator. The distance between the power electrode and counterelectrode can be varied between 5 and 30 mm. The discharge space is enclosed in the PTFE chamber with optical window. Both electrodes are enveloped with ribbed coolers that are externally chilled by an air fan. Argon (purity 99.996%, Messer Technogas, Czech Republic) is used as the working (plasma) gas and, at the same time, as an aerosol carrier. The Ar flow is controlled using a needle valve and the flow rate in the range 0.3–1.2 dm^3 min^{-1} was measured with a flowmeter. On some experiments, nitrogen (purity 99.99%, Linde Technoplyn, Czech Republic) was added up to the flow rate 0.8 dm^3 min^{-1}. As the low-power discharge is susceptible to extinguishing by introduction of aqueous aerosol and vapours, an ultrasonic nebulizer with desolvation unit U-5000 AT^+ (Cetac Technologies, U.S.A.) has been used for aerosol generation. The high-power plasma is not sensitive to water loading, and therefore, a customary concentric glass nebulizer (Meinhard Assoc., U.S.A.) without desolvation has been employed. Samples are delivered to nebulizers (1.5 cm^3 min^{-1}) with a peristaltic pump PCN 01 (Labeco

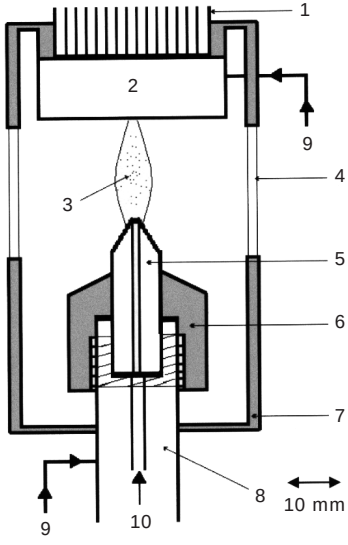

FIG. 2
Detailed view of the discharge chamber: 1 cooler, 2 counter-electrode, 3 discharge, 4 transparent window, 5 replaceable tip, 6 threaded nut, 7 Teflon wall, 8 jet-body, 9 RF feeding, 10 argon inlet

Ltd., Czech Republic). Working solutions were prepared from commercial standard stock solutions (p.a.) Astasol® (Analytika Ltd., Prague, Czech Republic)

Spectrometer

An emission spectrometer consisting of a commercial spectral apparatus, a detector and measuring devices was assembled in our laboratory[13]. Double monochromator GDM-1000 (Carl Zeiss, Jena, Germany) is provided with 2 planar gratings 90 × 110 mm (651 lines/mm) in Littrow mounting. Two concave mirrors with a focal length of 1 100 mm and effective diameter of 200 mm have been additionally alumetized. Monochromators are separated with a rotating modulator (25 Hz). A scattered light offset is $1.3 \cdot 10^{-12}$ at 572 nm. The scatter was measured with a He-Ne laser with the lasing wavelength 633 nm. The entrance and exit slits are 100 mm high and their width is adjustable between 0 and 3 mm with a step of 0.01 mm. The radius of the slit curvature is 1 520 mm. For the described measurements, the 0.1-mm slit width is used. The slit height is adjusted to 30 mm. Plasma is imaged (1 : 1) onto the slit by means of a single converging lens (f = 300 mm). The relative aperture number is D/f = 1 : 10.4. Theoretical resolution power in the 1st and 2nd spectral order is 117 000 and 234 000, respectively. The practical resolution powers 72 000 and 132 000 have been evaluated from the spectral profile of a He-Ne laser (1st order) and from the spectral profile of Ca 422.7-nm line emitted by a hollow cathode lamp (2nd order). The profile of Ca 422.7 nm emitted by the hollow cathode lamp has been obtained by measurement with a Fabry–Perrot interferometer[14]. The measurement range in the 1st and the 2nd order is 560–1 300 and 360–600 nm, respectively. The reciprocal linear dispersion is 0.7 nm in the 1st order. A red filter RG5 (Carl Zeiss, Jena, Germany) is used as the order sorter. A laboratory-assembled detection system is used. Synchronized (25 Hz) detection of radiation is performed using a photomultiplier M12FC51 with a multialkaline cathode of the S-20 type. The photomultiplier output voltage is amplified with a selective amplifier (25 Hz) provided with a synchronous detector No. 367 415.011.27/1 with a built-in high-voltage supply for the photomultiplier tube. The original input circuit has been replaced with an amplifier and transistor FET BF 245C with a common emitter (a gain value of 10). This modification diminishes the noise. The amplified output voltage is recorded with a chart recorder K-101 or its precise value is read out by means of a digital converter TEC-1. All the above components are products of Carl Zeiss, Jena, Germany.

RESULTS AND DISCUSSION

The *low-power* discharge is operated at a power 100 W and the Ar flow rate 0.3–0.9 $dm^3\ min^{-1}$. The plasma outflows from the inner space of the nozzle having a form of a column, as it is evident from Fig. 3. When changing the nozzle diameter from 0.5 to 1.5 mm, the width of the plasma column increases from 0.7 to 1.5 mm. The discharge length is determined by the distance between electrodes, which can be varied between 5 and 30 mm. Within these dimensions, the discharge remains stable. It has been found that the brass tip is more resistant to erosion due to the discharge than the graphite. The influence of nitrogen added into the chamber by separate

inlet was studied up to the flow 0.8 dm^3 min^{-1}. The flow of nitrogen 50 cm^3 min^{-1} was found sufficient for stabilizing the discharge in the axial position. The same effect can be obtained when the discharge burns in the atmosphere.

The vibrational temperature of the low-power RPJ is equal to 3 000 K, based on the intensity I of the molecular band of the 2nd positive system N_2 (wavelength λ = 365–383 nm), Fig. 4. Spectra of selected analytical lines of Li, Na, K, Rb, Ca, Ba, Al, In and Sc have been recorded using an ultra-

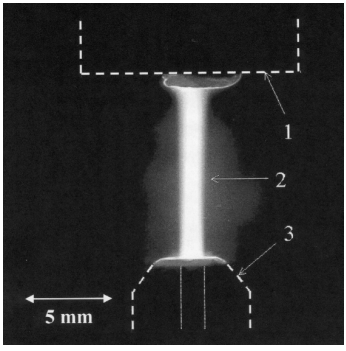

FIG. 3
Detailed photo of the plasma discharge: 1 counter-electrode, 2 discharge, 3 replaceable tip

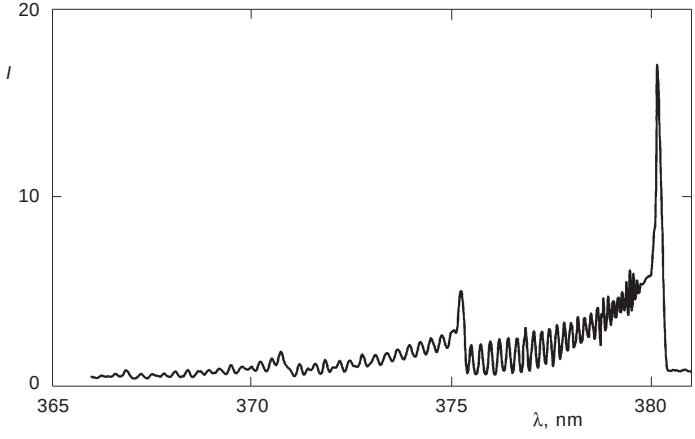

FIG. 4
Spectrum of the N_2 2nd positive system (365–383 nm) excited in the low-power RPJ discharge and used for the computation of vibrational temperature

sonic nebulizer at an argon flow rate of 0.9 dm^3 min^{-1}. Alkali metals are efficiently excited in the RPJ, as it is apparent from the spectrum of Li 670.784 nm at a concentration of 1 ng cm^{-3} of Li (Fig. 5). The observed atomic and ionic (II) spectral lines are presented together with limits of detection (x_D, 3σ) in Table II. It follows from comparison with x_D values for ICP–AES (ref.[15]), that the RPJ exhibits higher limits of detection both for atomic (I) and ionic (II) lines. This is due to considerably lower RPJ discharge temperature in comparison with an ICP source. Consequently, lower population of excited atoms and ions can be expected. The differences between ICP and RPJ limits of detection of alkali metals are not so wide because the populations of neutral atoms of alkali metals are depleted in an ICP due to their ionization. On the contrary, the degree of ionization in the RPJ discharge is expected to be several orders of magnitude lower in comparison with an ICP discharge, which explains enormously wide differences between limits of detection obtained with ionic lines. Generally, higher limits of detection obtained with the RPJ are perhaps also due to the absence of an analytical channel inside the discharge. Therefore, only a small portion of aerosol is in contact with the RPJ discharge.

The calibration curves obtained with ultrasonic nebulization for Li, K and Rb are presented in the log–log scale in Fig. 6. It implies from the slopes (greater than one) of linear plots for Li and Rb that the intensity *I vs* concentration ρ dependences are influenced by ionization interferences

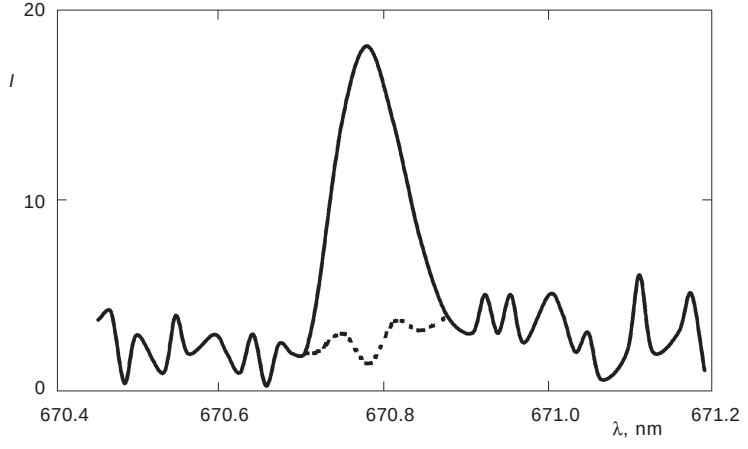

FIG. 5
Spectrum of the Li 670.784 nm line excited in the low-power RPJ; 1 ng cm^{-3} Li, ultrasonic nebulizer, 0.9 dm^3 min^{-1} Ar, forwarded power 100 W

TABLE II
Observed spectral lines and limits of detection (x_D, 3σ). ICP–AES is Model JY-138 Ultrace

Element	Line	λ, nm	x_D, ng cm^{-3} RPJ	x_D, ng cm^{-3} ICP–AES[a] (ref.[15])
Li	I	670.784	0.1	0.3
Na	I	588.995	30	0.4
Na	I	589.592	30	0.4
K	I	766.491	10	6
Rb	I	780.023	3	–
Ca	II	393.366	5	0.002
Ca	I	422.673	30	0.07
Ba	II	455.403	500	0.03
Ba	I	553.555	100	–
Al	I	396.153	300	0.13
In	I	451.131	30	20
Sc	I	391.181	2 000	0.06[b]
Eu	I	459.402	200	0.9[b]

[a] Model JY-38. [b] Lines: Sc II 361.384 nm, Eu II 381.967 nm; x_D values for atomic lines of Sc and Eu are not listed in ref.[15]

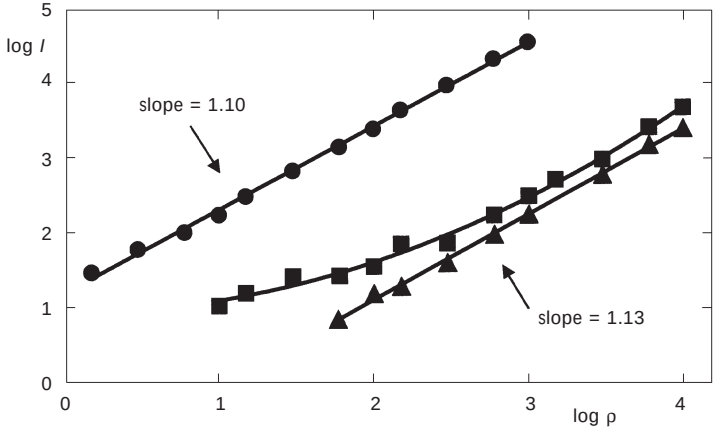

FIG. 6
Line intensity *vs* concentration (in ng cm^{-3}) dependences measured in the low-power RPJ; ultrasonic nebulization, 0.9 dm^3 min^{-1} Ar, forwarded power 100 W. ● Li 670.78, ■ K 766.49 and ▲ Rb 780.02 nm

(Fig. 6). The same is clear from even non-linear course of the curve for K (Fig. 6).

The *high-power* RPJ is operated at 200 W and exhibits stable behaviour at argon flow rates between 0.3–0.6 dm^3 min^{-1}. While the low-power RPJ is frequently extinguished at the introduction of non-desolvated aerosol, the

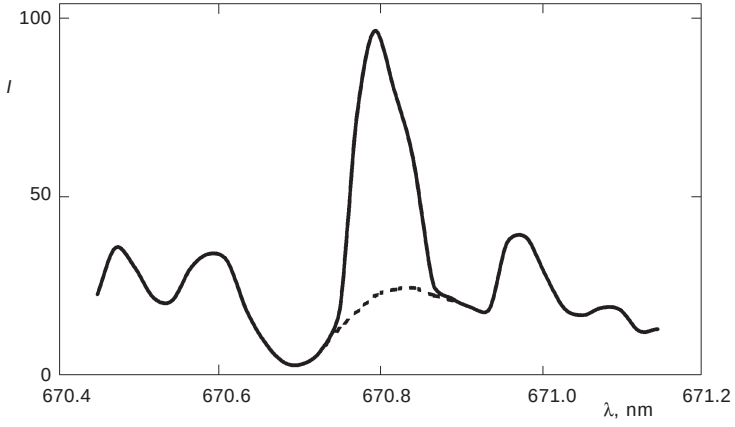

FIG. 7
Spectrum of the Li 670.784 nm line excited in the high-power RPJ; 100 ng cm^{-3} Li, concentric Meinhard nebulizer, 0.3 dm^3 min^{-1} Ar, forwarded power 200 W

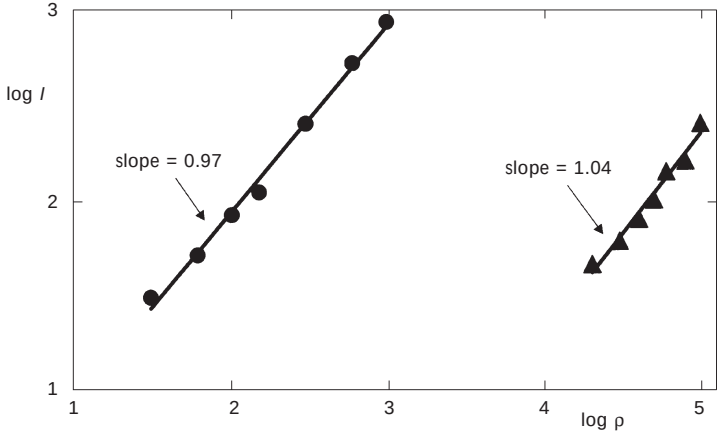

FIG. 8
Line intensity *vs* concentration (in ng cm^{-3}) dependences measured in the high-power RPJ; concentric Meinhard nebulizer, 0.3 dm^3 min^{-1} Ar, forwarded power 100 W. ● Li 670.78 and ▲ Rb 780.02 nm

high-power RPJ tolerates the aerosol from a Meinhard concentric nebulizer. Therefore, the use of a high-cost ultrasonic nebulizer can be circumvented. However, the efficiency of sample introduction with the Meinhard nebulizer is considerably lower than that with an ultrasonic nebulizer. The spectrum of Li 670.784 nm recorded at the concentration 100 ng cm^{-3} of Li (Fig. 7) and measurement of the blank solution yielded the limit of detection 8 ng cm^{-3} Li. Calibration curves obtained with a Meinhard nebulizer for Li and Rb are presented in the log–log scale in Fig. 8. Extension of calibrations to lower concentrations could be achieved with ultrasonic nebulization, which is the aim of our further study. Then a direct comparison between the two RPJ discharges will be possible.

CONCLUSION

Two high-frequency plasma-jet discharges (27.12 and 13.56 MHz) have been designed and put into operation. The possibility of their use in atomic emission spectrometry with introduction of aerosols has been studied. The 27.12 MHz/100 W discharge is stable only when desolvated aerosol is introduced. Limits of detection of Li, Na, K and Rb obtained with their atomic lines are of the order of ng cm^{-3}. Atomic and ionic (II) lines of Ca and Ba, and atomic lines of Al, In, Sc and Eu are also excited. However, their limits of detection are higher than in the ICP–AES with pneumatic nebulization. The non-linear course of calibration curves for Li, K and Rb demonstrates the influence of ionization interferences. The 13.56 MHz/200 W discharge is more robust and accepts aqueous aerosol generated by means of a concentric Meinhard nebulizer. Further development of both plasma sources towards their better stability by the aerosol introduction is necessary, which is the aim of our further work.

The authors gratefully acknowledge the Ministry of Education, Youth and Sports of the Czech Republic for a research grant "Laboratory of Plasma Sources for Chemical Analysis" (Projects No. VS 97020 and CEZ: J07/98:143100003). M. Štěpán and M. Semerád wish to thank Dr P. Krásenský, M.S. (Masaryk University Brno, Czech Republic) for the construction of the discharge chamber. M. Štěpán especially wishes to thank Dr P. Slavíček, M.S. (Department of Physical Electronics, Masaryk University Brno) for his collaboration in diagnostic measurements. Finally, we would like to express our thanks to the Central Institute for Supervising and Testing in Agriculture, Brno, Czech Republic, for the loan of an ultrasonic nebulizer.

REFERENCES

1. Reed T. B.: *J. Appl. Phys.* **1961**, *32*, 821.

2. Greenfield S., Jones I. L., Berry C. T.: *Analyst (Amsterdam)* **1964**, *89*, 713.
3. Wendt R. H., Fassel V. A.: *Anal. Chem.* **1965**, *37*, 920.
4. Beauchemin D., Le Blanc J. C. Y., Peters G. R., Persaud A. T.: *Anal. Chem.* **1994**, *66*, 462R.
5. Engel U., Bilgic A. M., Haase O., Voges E., Broekaert J. A. C.: *Anal. Chem.* **2000**, *72*, 193.
6. Bilgic A. M., Engel U., Voges E., Kuckelheim M., Broekaert J. A. C.: *Plasma Sources Sci. Technol.* **2000**, *9*, 1.
7. Bilgic A. M., Voges E., Engel U., Broekaert J. A. C.: *J. Anal. At. Spectrom.* **2000**, *15*, 579.
8. Kapička V., Klíma M., Vaculík R., Brablec A., Slavíček P., Střecha M., Šícha M.: *Czech. J. Phys.* **1998**, *48*, 1161.
9. Brablec A., Kapička V., Ondráček Z., Slavíček P., Střecha M., Šťastný F., Vaculík R.: *Czech. J. Phys.* **1999**, *49*, 329.
10. Kapička V., Šícha M., Klíma M., Hubička Z., Touš J., Brablec A., Slavíček P., Behnke J. F., Tichý M., Vaculík R.: *Plasma Sources Sci. Technol.* **1999**, *8*, 15.
11. Janča J., Klíma M., Slavíček P., Zajíčková L.: *Surf. Coat. Technol.* **1999**, *116–119*, 547.
12. Štěpán M., Otruba V., Kanický V.: *ICP Information Newsletter* **2000**, *26*, 143.
13. Otruba V., Sommer L.: *Fresenius' J. Anal. Chem.* **1989**, *335*, 887.
14. Otruba V., Jambor J., Horák J.: *Chem. Listy* **1979**, *73*, 295.
15. *Instruction Manual*. Jobin–Yvon, Sa., Longjumeau (France) 1999.